23 December 1983, Volume 222, Number 4630 SCIENCE

Nuclear Winter: Global Consequences of Multiple Nuclear Explosions

R. P. Turco, O. B. Toon, T. P. Ackerman
J. B. Pollack, Carl Sagan

Summary. The potential global atmospheric and climatic consequences of nuclear war are investigated using models previously developed to study the effects of volcanic eruptions. Although the results are necessarily imprecise, due to a wide range of possible scenarios and uncertainty in physical parameters, the most probable first-order effects are serious. Significant hemispherical attenuation of the solar radiation flux and subfreezing land temperatures may be caused by fine dust raised in high-yield nuclear surface bursts and by smoke from city and forest fires ignited by airbursts of all yields. For many simulated exchanges of several thousand megatons, in which dust and smoke are generated and encircle the earth within 1 to 2 weeks, average light levels can be reduced to a few percent of ambient and land temperatures can reach −15° to −25°C. The yield threshold for major optical and climatic consequences may be very low: only about 100 megatons detonated over major urban centers can create average hemispheric smoke optical depths greater than 2 for weeks and, even in summer, subfreezing land temperatures for months. In a 5000-megaton war, at northern mid-latitude sites remote from targets, radioactive fallout on time scales of days to weeks can lead to chronic mean doses of up to 50 rads from external whole-body gamma-ray exposure, with a likely equal or greater internal dose from biologically active radionuclides. Large horizontal and vertical temperature gradients caused by absorption of sunlight in smoke and dust clouds may greatly accelerate transport of particles and radioactivity from the Northern Hemisphere to the Southern Hemisphere. When combined with the prompt destruction from nuclear blast, fires, and fallout and the later enhancement of solar ultraviolet radiation due to ozone depletion, long-term exposure to cold, dark, and radioactivity could pose a serious threat to human survivors and to other species.

Concern has been raised over the short- and long-term consequences of the dust, smoke, radioactivity, and toxic vapors that would be generated by a nuclear war (*1–7*). The discovery that dense clouds of soil particles may have played a major role in past mass extinctions of life on Earth (*8–10*) has encouraged the reconsideration of nuclear war effects. Also, Crutzen and Birks (*7*) recently suggested that massive fires ignited by nuclear explosions could generate quantities of sooty smoke that would attenuate sunlight and perturb the climate. These developments have led us to calculate, using new data and improved models, the potential global environmental effects of dust and smoke clouds (henceforth referred to as nuclear dust and nuclear smoke) generated in a nuclear war (*11*). We neglect the short-term effects of blast, fire, and radiation (*12–14*). Most of the world's population could probably survive the initial nuclear exchange and would inherit the postwar environment. Accordingly, the longer-term and global-scale aftereffects of nuclear war might prove to be as important as the immediate consequences of the war.

To study these phenomena, we used a series of physical models: a nuclear war scenario model, a particle microphysics model, and a radiative-convective model. The nuclear war scenario model specifies the altitude-dependent dust, smoke, radioactivity, and NO_x injections for each explosion in a nuclear exchange (assuming the size, number, and type of detonations, including heights of burst, geographic locales, and fission yield fractions). The source model parameterization is discussed below and in a more detailed report (*15*). The one-dimensional microphysical model (*15–17*) predicts the temporal evolution of dust and smoke clouds, which are taken to be rapidly and uniformly dispersed. The one-dimensional radiative-convective model (1-D RCM) uses the calculated dust and smoke particle size distributions and optical constants and Mie theory to calculate visible and infrared optical properties, light fluxes, and air temperatures as a function of time and height. Because the calculated air temperatures are sensitive to surface heat capacities, separate simulations are performed for land and ocean environments, to define possible temperature contrasts. The techniques used in our 1-D RCM calculations are well documented (*15, 18*).

Although the models we used can provide rough estimates of the average effects of widespread dust and smoke clouds, they cannot accurately forecast short-term or local effects. The applicability of our results depends on the rate and extent of dispersion of the explosion clouds and fire plumes. Soon after a large nuclear exchange, thousands of individual dust and smoke clouds would be distributed throughout the northern mid-latitudes and at altitudes up to 30 km.

R. P. Turco is at R & D Associates, Marina del Rey, California 90291; O. B. Toon, T. P. Ackerman, and J. B. Pollack are at NASA Ames Research Center, Moffett Field, California 94035; and Carl Sagan is at Cornell University, Ithaca, New York 14853.

Downloaded from www.sciencemag.org on April 23, 2014

Horizontal turbulent diffusion, vertical wind shear, and continuing smoke emission could spread the clouds of nuclear debris over the entire zone, and tend to fill in any holes in the clouds, within 1 to 2 weeks. Spatially averaged simulations of this initial period of cloud spreading must be viewed with caution; effects would be smaller at some locations and larger at others, and would be highly variable with time at any given location.

The present results also do not reflect the strong coupling between atmospheric motions on all length scales and the modified atmospheric solar and infrared heating and cooling rates computed with the 1-D RCM. Global circulation patterns would almost certainly be altered in response to the large disturbances in the driving forces calculated here (*19*). Although the 1-D RCM can predict only horizontally, diurnally, and seasonally averaged conditions, it is capable of estimating the first-order climate responses of the atmosphere, which is our intention in this study.

Scenarios

A review of the world's nuclear arsenals (*20–24*) shows that the primary strategic and theater weapons amount to $\simeq$ 12,000 megatons (MT) of yield carried by $\simeq$ 17,000 warheads. These arsenals are roughly equivalent in explosive power to 1 million Hiroshima bombs. Although the total number of high-yield warheads is declining with time, about 7000 MT is still accounted for by warheads of > 1 MT. There are also $\simeq$ 30,000 lower-yield tactical warheads and munitions which are ignored in this analysis. Scenarios for the possible use of nuclear weapons are complex and controversial. Historically, studies of the long-term effects of nuclear war have focused on a full-scale exchange in the range of 5000 to 10,000 MT (*2, 12, 20*). Such exchanges are possible, given the current arsenals and the unpredictable nature of warfare, particularly nuclear warfare, in which escalating massive exchanges could occur (*25*).

An outline of the scenarios adopted here is presented in Table 1. Our baseline scenario assumes an exchange of 5000 MT. Other cases span a range of total yield from 100 to 25,000 MT. Many high-priority military and industrial assets are located near or within urban zones (*26*). Accordingly, a modest fraction (15 to 30 percent) of the total yield is assigned to urban or industrial targets. Because of the large yields of strategic warheads [generally $\gtrsim$ 100 kilotons (KT)], "surgical" strikes against individual targets are difficult; for instance, a 100-KT airburst can level and burn an area of $\simeq$ 50 km^2, and a 1-MT airburst, $\simeq$ 5 times that area (*27, 28*), implying widespread collateral damage in any "countervalue," and many "counterforce," detonations.

Table 1. Nuclear exchange scenarios.

Case*	Total yield (MT)	Percent of yield		Warhead yield range (MT)	Total number of explosions
		Surface bursts	Urban or industrial targets		
1. Baseline exchange	5,000	57	20	0.1 to 10	10,400
2. Low-yield airbursts	5,000	10	33	0.1 to 1	22,500†
9. 10,000-MT‡ maximum	10,000	63	15	0.1 to 10	16,160
10. 3,000-MT exchange	3,000	50	25	0.3 to 5	5,433
11. 3,000-MT counterforce	3,000	70	0	1 to 10	2,150
12. 1,000-MT exchange§	1,000	50	25	0.2 to 1	2,250
13. 300-MT Southern Hemisphere‖	300	0	50	1.	300
14. 100-MT city attack¶	100	0	100	0.1	1,000
16. Silos, "severe" case#	5,000	100	0	5 to 10	700
18. 25,000-MT‡ "future war"	25,000	72	10	0.1 to 10	28,300†

*Case numbers correspond to a complete list given in (*15*). Detailed detonation inventories are not reproduced here. Except as noted, attacks are concentrated in the NH. Baseline dust and smoke parameters are described in Tables 2 and 3. †Assumes more extensive MIRVing of existing missiles and some possible new deployment of medium- and long-range missiles (*20–23*). ‡Although these larger total yields might imply involvement of the entire globe in the war, for ease of comparison hemispherically averaged results are still considered. §Nominal area of wildfires is reduced from 5×10^5 to 5×10^4 km^2. ‖Nominal area of wildfires is reduced from 5×10^5 to 5×10^3 km^2. ¶The central city burden of combustibles is 20 g/cm^2 (twice that in the baseline case) and the net fire smoke emission is 0.026 g per gram of material burned. There is a negligible contribution to the opacity from wildfires and dust. #Includes a sixfold increase in the fine dust mass lofted per megaton of yield.

The properties of nuclear dust and smoke are critical to the present analysis. The basic parameterizations are described in Tables 2 and 3, respectively; details may be found in (*15*). For each explosion scenario, the fundamental quantities that must be known to make optical and climate predictions are the total atmospheric injections of fine dust ($\lesssim$ 10 μm in radius) and soot.

Nuclear explosions at or near the ground can generate fine particles by several mechanisms (*27*): (i) ejection and disaggregation of soil particles (*29*), (ii) vaporization and renucleation of earth and rock (*30*), and (iii) blowoff and sweepup of surface dust and smoke (*31*). Analyses of nuclear test data indicate that roughly 1×10^5 to 6×10^5 tons of dust per megaton of explosive yield are held in the stabilized clouds of land surface detonations (*32*). Moreover, size analysis of dust samples collected in nuclear clouds indicates a substantial submicrometer fraction (*33*). Nuclear surface detonations may be much more efficient in generating fine dust than volcanic eruptions (*15, 34*), which have been used inappropriately in the past to estimate the impacts of nuclear war (*2*).

The intense light emitted by a nuclear fireball is sufficient to ignite flammable materials over a wide area (*27*). The explosions over Hiroshima and Nagasaki both initiated massive conflagrations (*35*). In each city, the region heavily damaged by blast was also consumed by fire (*36*). Assessments over the past two decades strongly suggest that widespread fires would occur after most nuclear bursts over forests and cities (*37–44*). The Northern Hemisphere has $\simeq 4 \times 10^7$ km^2 of forest land, which holds combustible material averaging $\sim$ 2.2 g/cm^2 (*7*). The world's urban and suburban zones cover an area of $\simeq 1.5 \times 10^6$ km^2 (*15*). Central cities, which occupy 5 to 10 percent of the total urban area, hold $\simeq$ 10 to 40 g/cm^2 of combustible material, while residential areas hold $\simeq$ 1 to 5 g/cm^2 (*41, 42, 44, 45*). Smoke emissions from wildfires and large-scale urban fires probably lie in the range of 2 to 8 percent by mass of the fuel burned (*46*). The highly absorbing sooty fraction (principally graphitic carbon) could comprise up to 50 percent of the emission by weight (*47, 48*). In wildfires, and probably urban fires, $\gtrsim$ 90 percent of the smoke mass consists of particles < 1 μm in radius (*49*). For calculations at visible wavelengths, smoke particles are assigned an imaginary part of the refractive index of 0.3 (*50*).

Simulations

The model predictions discussed here generally represent effects averaged over the Northern Hemisphere (NH). The initial nuclear explosions and fires would be largely confined (*51*) to northern mid-latitudes (30° to 60°N). Accordingly, the predicted mean dust and smoke opacity could be larger by a factor of 2 to 3 at mid-latitudes, but smaller elsewhere. Hemispherically averaged optical depths at visible wavelengths (*52*) for the mixed nuclear dust and smoke clouds corresponding to the scenarios in Table 1 are shown in Fig. 1. The vertical optical depth is a convenient diagnostic of nuclear cloud properties and may be used roughly to scale atmospheric light levels and temperatures for the various scenarios.

In the baseline scenario (case 1, 5000 MT), the initial NH optical depth is $\simeq 4$, of which $\simeq 1$ is due to stratospheric dust and $\simeq 3$ to tropospheric smoke. After 1 month the optical depth is still $\simeq 2$. Beyond 2 to 3 months, dust dominates the optical effects, as the soot is largely depleted by rainout and washout (*54*). In the baseline case, about 240,000 km^2 of urban area is partially (50 percent) burned by $\simeq$ 1000 MT of explosions (only 20 percent of the total exchange yield). This roughly corresponds to one sixth of the world's urbanized land area, one fourth of the developed area of the NH, and one half of the area of urban centers with populations > 100,000 in the NATO and Warsaw Pact countries. The mean quantity of combustible material consumed over the burned area is $\simeq 1.9$ g/cm^2. Wildfires ignited by the remaining 4000 MT of yield burn another 500,000 km^2 of forest, brush, and grasslands (*7, 39, 55*), consuming $\simeq 0.5$ g/cm^2 of fuel in the process (*7*).

Total smoke emission in the baseline case is $\simeq$ 225 million tons (released over several days). By comparison, the current annual global smoke emission is estimated as $\simeq$ 200 million tons (*15*), but is probably < 1 percent as effective as nuclear smoke would be in perturbing the atmosphere (*56*).

The optical depth simulations for cases 1, 2, 9, and 10 in Fig. 1 show that a range of exchanges between 3000 and 10,000 MT might create similar effects. Even cases 11, 12, and 13, while less severe in their absolute impact, produce optical depths comparable to or exceeding those of a major volcanic eruption. It is noteworthy that eruptions such as Tambora in 1815 may have produced significant climate perturbations, even with an average surface temperature decrease of $\lesssim 1$ K (*57–60*).

Case 14 represents a 100-MT attack on cities with 1000 100-KT warheads. In the attack, 25,000 km^2 of built-up urban area is burned (such an area could be accounted for by $\simeq$ 100 major cities). The smoke emission is computed with fire parameters that differ from the baseline case. The average burden of combustible material in city centers is 20 g/cm^2 (versus 10 g/cm^2 in case 1) and the average smoke emission factor is 0.026 gram of smoke per gram of material burned (versus the conservative figure of 0.011 g/g adopted for central city fires in the baseline case). About 130 million tons of urban smoke is injected into the troposphere in each case (none reaches the stratosphere in case 14). In the baseline case, only about 10 percent of the urban smoke originates from fires in city centers (Table 3).

The smoke injection threshold for ma-

Table 2. Dust parameterization for the baseline case.

Type of burst	Dust mass (ton/MT):	Dust size distribution† [r_m(μm)/σ/α]:	H_2O (ton/MT):
	*Materials in stabilized nuclear explosion clouds**		
Land surface	3.3×10^5	0.25/2.0/4.0	1.0×10^5
Land near-surface	1.0×10^5	0.25/2.0/4.0	1.0×10^5

Dust composition: siliceous minerals and glasses

Index of refraction at visible wavelengths‡: $n = 1.50 - 0.001\,i$

Stabilized nuclear cloud top and bottom heights, z_t and z_b, for surface and low-air bursts§: $z_t = 21\ Y^{0.2}$; $z_b = 13\ Y^{0.2}$; where Y = yield in megatons

Multiburst interactions are ignored

Baseline dust injections

Total dust $\simeq 9.6 \times 10^8$ tons; 80 percent in the stratosphere; 8.4 percent < 1 μm in radius

Submicrometer dust injection is ~ 25 ton/KT for surface bursts, which represents ~ 0.5 percent of the total ejecta mass

Total initial area of stabilized fireballs $\simeq 2.0 \times 10^6$ km^2

*Materials are assumed to be uniformly distributed in the clouds. †Particle size distributions (number/cm^3 − μm radius) are log-normal with a power-law tail at large sizes. The parameters r_m and σ are the log-normal number mode radius and size variance, respectively, and α is the exponent of the $r^{-\alpha}$ dependence at large sizes. The log-normal and power-law distributions are connected at a radius of ≅ 1 μm (*15*). ‡The refractive indices of dust at infrared wavelengths are discussed in (*10*). §The model of Foley and Ruderman (*87*) is adopted, but with the cloud heights lowered by about 0.5 km. The original cloud heights are based on U.S. Pacific test data, and may overestimate the heights at mid-latitudes by several kilometers.

Table 3. Fire and smoke parameterization for the baseline case.

Fire area and emissions

Area of urban fire ignition defined by the 20 cal/cm^2 thermal irradiance contour ($\simeq$ 5 psi peak overpressure contour) with an average atmospheric transmittance of 50 percent: A (km^2) = 250 Y, where Y = yield in megatons detonated over cities; overlap of fire zones is ignored

Urban flammable material burdens average 3 g/cm^2 in suburban areas and 10 g/cm^2 in city centers (5 percent of the total urban area)

Average consumption of flammables in urban fires is 1.9 g/cm^2

Average net smoke emission factor is 0.027 g per gram of material burned (for urban centers it is only 0.011 g/g)

Area of wildfires is 5×10^5 km^2 with 0.5 g/cm^2 of fuel burned, and a smoke emission factor of 0.032 g/g

Long-term fires burn 3×10^{14} g of fuel with an emission factor of 0.05 g/g

Fire plume heights (top and bottom altitudes)

Urban fires: 1 to 7 km

Fire storms (5 percent of urban fires): $z_b \leq 5$ km; $z_t \leq 19$ km

Wildfires: 1 to 5 km

Long-term fires: 0 to 2 km

Fire duration

Urban fires, 1 day; wildfires, 10 days; long-term fires, 30 days

Smoke properties

Density, 1.0 g/cm^3; complex index of refraction, $1.75 - 0.30\,i$; size distribution, log-normal with r_m(μm)/σ = 0.1/2.0 for urban fires and 0.05/2.0 for wildfires and long-term fires

Baseline smoke injections

Total smoke emission = 2.25×10^8 tons, 5 percent in the stratosphere

Urban-suburban fires account for 52 percent of emissions, fire storms for 7 percent, wildfires for 34 percent, and long-term fires for 7 percent

Total area burned by urban-suburban fires is 2.3×10^5 km^2; fire storms, 1.2×10^4 km^2; and wildfires, 5.0×10^5 km^2

jor optical perturbations on a hemispheric scale appears to lie at $\simeq 1 \times 10^8$ tons. From case 14, one can envision the release of $\simeq 1 \times 10^6$ tons of smoke from each of 100 major city fires consuming $\simeq 4 \times 10^7$ tons of combustible material per city. Such fires could be ignited by 100 MT of nuclear explosions. Unexpectedly, less than 1 percent of the existing strategic arsenals, if targeted on cities, could produce optical (and climatic) disturbances much larger than those previously associated with a massive nuclear exchange of $\simeq$ 10,000 MT (*2*).

Figure 2 shows the surface temperature perturbation over continental land areas in the NH calculated from the dust and smoke optical depths for several scenarios. Most striking are the extremely low temperatures occurring within 3 to 4 weeks after a major exchange. In the baseline 5000-MT case, a minimum land temperature of $\simeq$ 250 K (−23°C) is predicted after 3 weeks. Subfreezing temperatures persist for several months. Among the cases shown, even the smallest temperature decreases on land are $\simeq$ 5° to 10°C (cases 4, 11, and 12), enough to turn summer into winter. Thus, severe climatological consequences might be expected in each of these cases. The 100-MT city airburst scenario (case 14) produces a 2-month interval of subfreezing land temperatures, with a minimum again near 250 K. The temperature recovery in this instance is hastened by the absorption of sunlight in optically thin remnant soot clouds (see below). Comparable exchanges with and without smoke emission (for instance, cases 10 and 11) show that the tropospheric soot layers cause a sudden surface cooling of short duration, while fine stratospheric dust is responsible for prolonged cooling lasting a year or more. [Climatologically, a long-term surface cooling of only 1°C is significant (*60*).] In all instances, nuclear dust acts to cool the earth's surface; soot also tends to cool the surface except when the soot cloud is both optically thin and located near the surface [an unimportant case because only relatively small transient warmings $\lesssim$ 2 K can thereby be achieved (*61*)].

Predicted air temperature variations over the world's oceans associated with changes in atmospheric radiative transport are always small (cooling of $\lesssim$ 3 K) because of the great heat content and rapid mixing of surface waters. However, variations in atmospheric zonal circulation patterns (see below) might significantly alter ocean currents and upwelling, as occurred on a smaller scale recently in the Eastern Pacific (El Niño) (*62*). The oceanic heat reservoir would also moderate the predicted continental land temperature decreases, particularly in coastal regions (*10*). The effect is difficult to assess because disturbances in atmospheric circulation patterns are likely. Actual temperature decreases in continental interiors might be roughly 30 percent smaller than predicted here, and along coastlines 70 percent smaller (*10*). In the baseline case, therefore, continental temperatures may fall to $\simeq$ 260 K before returning to ambient.

Predicted changes in the vertical temperature profile for the baseline nuclear exchange are illustrated as a function of time in Fig. 3. The dominant features of the temperature perturbation are a large warming (up to 80 K) of the lower stratosphere and upper troposphere, and a large cooling (up to 40 K) of the surface and lower troposphere. The warming is caused by absorption of solar radiation in the upper-level dust and smoke clouds; it persists for an extended period because of the long residence time of the particles at high altitudes. The size of the warming is due to the low heat capacity of the upper atmosphere, its small infrared emissivity, and the initially low temperatures at high altitudes. The surface cooling is the result of attenuation of the incident solar flux by the aerosol clouds (see Fig. 4) during the first month of the simulation. The greenhouse effect no longer occurs in our calculations because

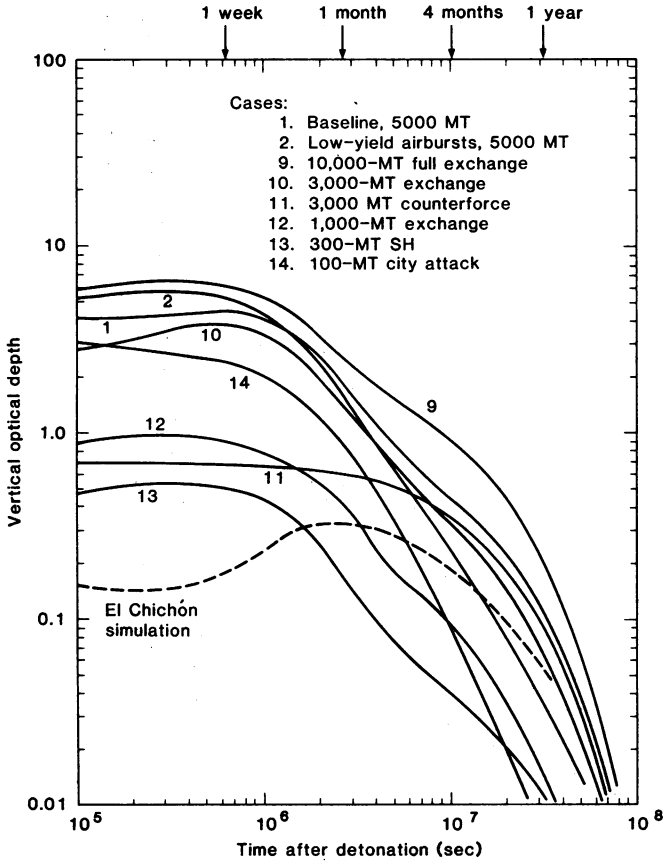

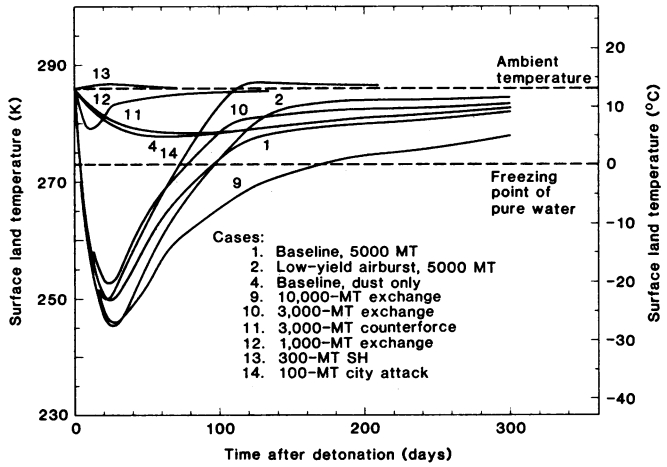

Fig. 1 (left). Time-dependent hemispherically averaged vertical optical depths (scattering plus absorption) of nuclear dust and smoke clouds at a wavelength of 550 nm. Optical depths $\lesssim$ 0.1 are negligible, $\sim$ 1 are significant, and $>$ 2 imply possible major consequences. Transmission of sunlight becomes highly nonlinear at optical depths $\gtrsim$ 1. Results are given for several of the cases in Table 1. Calculated optical depths for the expanding El Chichón eruption cloud are shown for comparison (*53*). Fig. 2 (right). Hemispherically averaged surface temperature variations after a nuclear exchange. Results are shown for several of the cases in Table 1. (Note the linear time scale, unlike that in Fig. 1). Temperatures generally apply to the interior of continental land masses. Only in cases 4 and 11 are the effects of fires neglected.

solar energy is deposited above the height at which infrared energy is radiated to space.

Decreases in insolation for several nuclear war scenarios are shown in Fig. 4. The baseline case implies average hemispheric solar fluxes at the ground $\lesssim 10$ percent of normal values for several weeks (apart from any patchiness in the dust and smoke clouds). In addition to causing the temperature declines mentioned above, the attenuated insolation could affect plant growth rates, and vigor in the marine (*63*), littoral, and terrestrial food chains. In the 10,000-MT "severe" case, average light levels are below the minimum required for photosynthesis for about 40 days over much of the Northern Hemisphere. In a number of other cases, insolation may, for more than 2 months, fall below the compensation point at which photosynthesis is just sufficient to maintain plant metabolism. Because nuclear clouds are likely to remain patchy the first week or two after an exchange, leakage of sunlight through holes in the clouds could enhance plant growth activity above that predicted for average cloud conditions; however, soon thereafter the holes are likely to be sealed.

Sensitivity Tests

A large number of sensitivity calculations were carried out as part of this study (*15*). The results are summarized here. Reasonable variations in the nuclear dust parameters in the baseline scenario produce initial hemispherically averaged dust optical depths varying from about 0.2 to 3.0. Accordingly, nuclear dust alone could have a major climatic impact. In the baseline case, the dust opacity is much greater than the total aerosol opacity associated with the El Chichón and Agung eruptions (*59, 64*); even when the dust parameters are assigned their least adverse values within the plausible range, the effects are comparable to those of a major volcanic explosion.

Figure 5 compares nuclear cloud optical depths for several variations of the baseline model smoke parameters (with dust included). In the baseline case, it is assumed that fire storms inject only a small fraction ($\simeq 5$ percent) of the total smoke emission into the stratosphere (*65*). Thus, case 1 and case 3 (no firestorms) are very similar. As an extreme excursion, all the nuclear smoke is injected into the stratosphere and rapidly dispersed around the globe (case 26); large optical depths can then persist for a year (Fig. 5). Prolongation of optical effects is also obtained in case 22, where the tropospheric washout lifetime of smoke particles is increased from 10 to 30 days near the ground. By contrast, when the nuclear smoke is initially contained near the ground and dynamical and hydrological removal processes are assumed to be unperturbed, smoke depletion occurs much faster (case 25). But even in this case, some of the smoke still diffuses to the upper troposphere and remains there for several months (*66*).

In a set of optical calculations, the imaginary refractive index of the smoke was varied between 0.3 and 0.01. The optical depths calculated for indices between 0.1 and 0.3 show virtually no differences (cases 1 and 27 in Fig. 5). At an index of 0.05, the absorption optical depth (*52*) is reduced by only $\simeq 50$ percent, and at 0.01, by $\simeq 85$ percent. The overall opacity (absorption plus scattering), moreover, increases by $\simeq 5$ percent. These results show that light absorption and heating in nuclear smoke clouds remain high until the graphitic carbon fraction of the smoke falls below a few percent.

One sensitivity test (case 29, not illustrated) considers the optical effects in the Southern Hemisphere (SH) of dust and soot transported from the NH stratosphere. In this calculation, the smoke in the 300-MT SH case 13 is combined with half the baseline stratospheric dust and smoke (to approximate rapid global dispersion in the stratosphere). The initial optical depth is $\simeq 1$ over the SH, dropping to about 0.3 in 3 months. Predicted average SH continental surface temperatures fall by 8 K within several weeks and remain at least 4 K below normal for nearly 8 months. The seasonal influence should be taken into account, however. For example, the worst consequences for the NH might result from a spring or

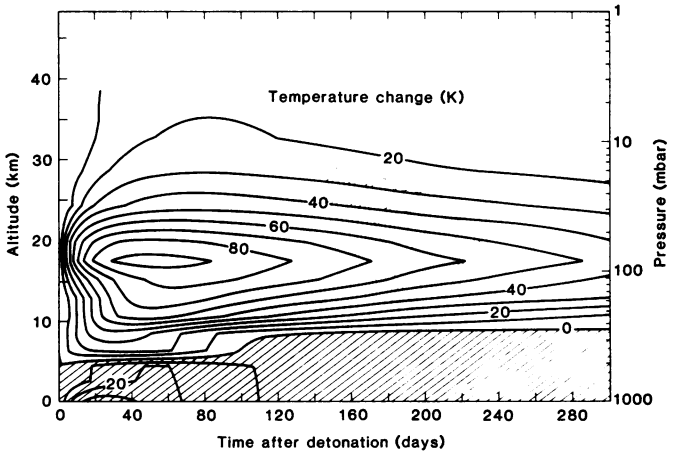

Fig. 3. Northern Hemisphere troposphere and stratosphere temperature perturbations (in Kelvins; 1 K = 1°C) after the baseline nuclear exchange (case 1). The hatched area indicates cooling. Ambient pressure levels in millibars are also given.

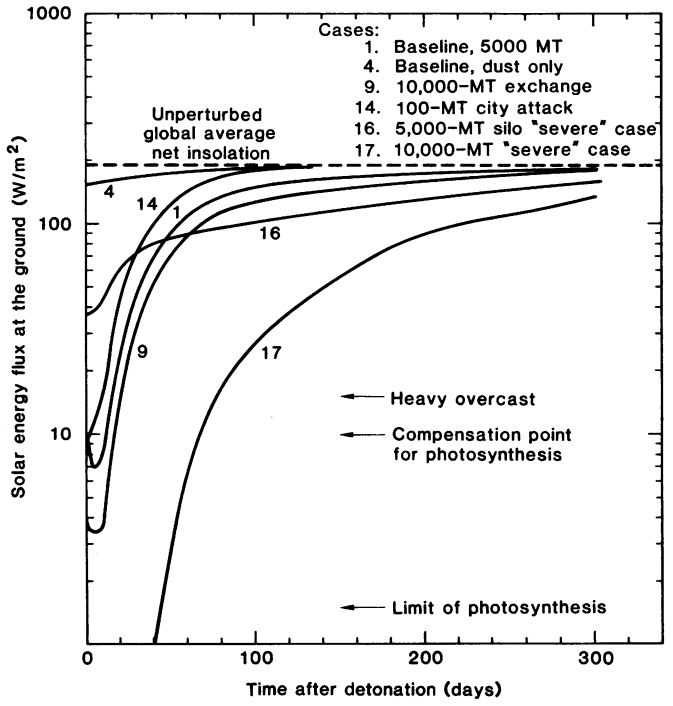

Fig. 4. Solar energy fluxes at the ground over the Northern Hemisphere in the aftermath of a nuclear exchange. Results are given for several of the cases in Table 1. (Note the linear time scale.) Solar fluxes are averaged over the diurnal cycle and over the hemisphere. In cases 4 and 16 fires are neglected. Also indicated are the approximate flux levels at which photosynthesis cannot keep pace with plant respiration (compensation point) and at which photosynthesis ceases. These limits vary for different species.

summer exchange, when crops are vulnerable and fire hazards are greatest. The SH, in its fall or winter, might then be least sensitive to cooling and darkening. Nevertheless, the implications of this scenario for the tropical regions in both hemispheres appear to be serious and worthy of further analysis. Seasonal factors can also modulate the atmospheric response to perturbations by smoke and dust, and should be considered.

A number of sensitivity tests for more severe cases were run with exchange yields ranging from 1000 to 10,000 MT and smoke and dust parameters assigned more adverse, but not implausible, values. The predicted effects are substantially worse (see below). The lower probabilities of these severe cases must be weighed against the catastrophic outcomes which they imply. It would be prudent policy to assess the importance of these scenarios in terms of the product of their probabilities and the costs of their corresponding effects. Unfortunately, we are unable to give an accurate quantitative estimate of the relevant probabilities. By their very nature, however, the severe cases may be the most important to consider in the deployment of nuclear weapons.

With these reservations, we present the optical depths for some of the more severe cases in Fig. 6. Large opacities can persist for a year, and land surface temperatures can fall to 230 to 240 K, about 50 K below normal. Combined with low light levels (Fig. 4), these severe scenarios raise the possibility of widespread and catastrophic ecological consequences.

Two sensitivity tests were run to determine roughly the implications for optical properties of aerosol agglomeration in the early expanding clouds. (The simulations already take into account continuous coagulation of the particles in the dispersed clouds.) Very slow dispersion of the initial stabilized dust and smoke clouds, taking nearly 8 months to cover the NH, was assumed. Coagulation of particles reduced the average opacity after 3 months by about 40 percent. When the adhesion efficiency of the colliding particles was also maximized, the average opacity after 3 months was reduced by $\simeq$ 75 percent. In the most likely situation, however, prompt agglomeration and coagulation might reduce the average hemispheric cloud optical depths by 20 to 50 percent.

Other Effects

We also considered, in less detail, the long-term effects of radioactive fallout, fireball-generated NO_x, and pyrogenic toxic gases (*15*). The physics of radioactive fallout is well known (*2, 5, 12, 27, 67*). Our calculations bear primarily on the widespread intermediate time scale accumulation of fallout due to washout and dry deposition of dispersed nuclear dust (*68*). To estimate possible exposure

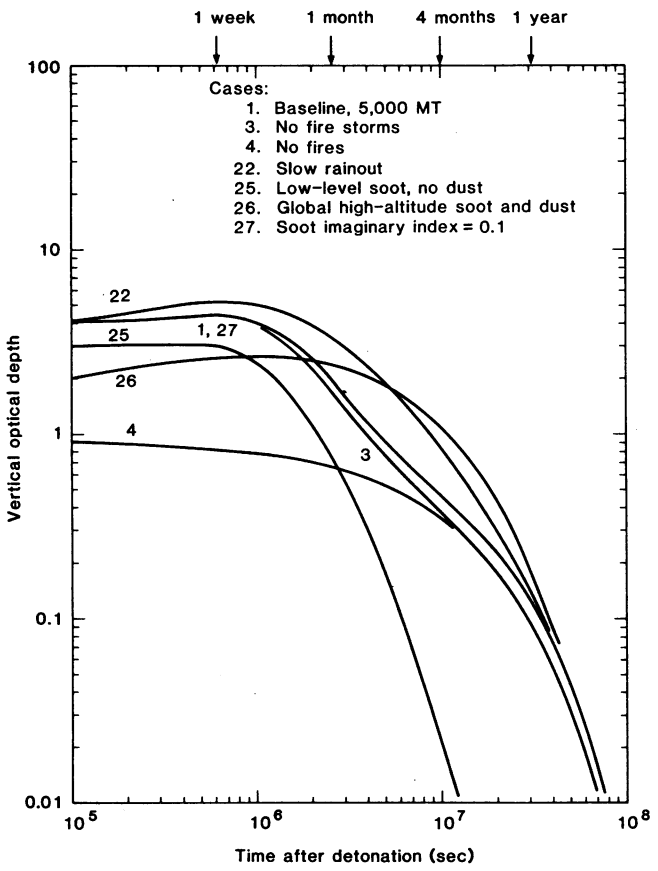

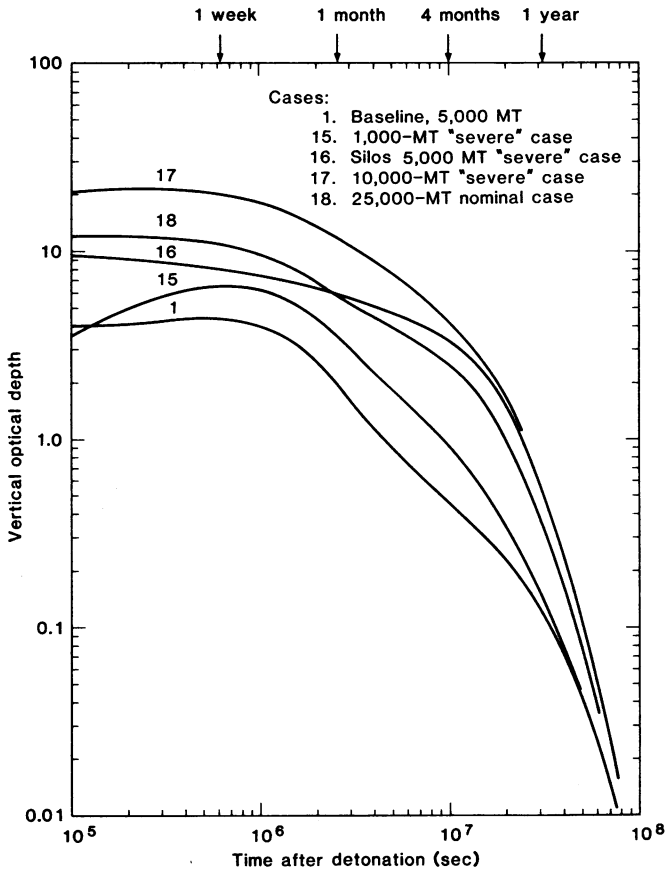

Fig. 5 (left). Time-dependent vertical optical depths (absorption plus scattering at 550 nm) of nuclear clouds, in a sensitivity analysis. Optical depths are average values for the Northern Hemisphere. All cases shown correspond to parameter variations of the baseline model (case 1) and include dust appropriate to it: case 3, no fire storms; case 4, no fires; case 22, smoke rainout rate decreased by a factor of 3; case 25, smoke initially confined to the lowest 3 km of the atmosphere; case 26, smoke initially distributed between 13 and 19 km over the entire globe; and case 27, smoke imaginary part of refractive index reduced from 0.3 to 0.1. For comparison, in case 4, only dust from the baseline model is considered (fires are ignored). Fig. 6 (right). Time-dependent vertical optical depths (absorption plus scattering at 550 nm) for enhanced cases of explosion yield or nuclear dust and smoke production. Conditions are detailed elsewhere (*15*). Weapon yield inventories are identical to the nominal cases of the same total yield described in Table 1 (cases 16 and 18 are also listed there). The "severe" cases generally include a sixfold increase in fine dust injection and a doubling of smoke emission. In cases 15, 17, and 18, smoke causes most of the opacity during the first 1 to 2 months. In cases 17 and 18, dust makes a major contribution to the optical effects beyond 1 to 2 months. In case 16, fires are neglected and dust from surface bursts produces all of the opacity.

levels, we adopt a fission yield fraction of 0.5 for all weapons. For exposure to only the gamma emission of radioactive dust that begins to fall out after 2 days in the baseline scenario (5000 MT), the hemispherically averaged total dose accumulated by humans over several months could be ≃ 20 rads, assuming no shelter from or weathering of the dust. Fallout during this time would be confined largely to northern mid-latitudes; hence the dose there could be ≃ 2 to 3 times larger (*69, 70*). Considering ingestion of biologically active radionuclides (*27, 71*) and occasional exposure to localized fallout, the average total chronic mid-latitude dose of ionizing radiation for the baseline case could be ≳ 50 rads of whole-body external gamma radiation, plus ≳ 50 rads to specific body organs from internal beta and gamma emitters (*71, 72*). In a 10,000-MT exchange, under the same assumptions, these mean doses would be doubled. Such doses are roughly an order of magnitude larger than previous estimates, which neglected intermediate time scale washout and fallout of tropospheric nuclear debris from low-yield (< 1-MT) detonations.

The problem of NO_x produced in the fireballs of high-yield explosions, and the resulting depletion of stratospheric ozone, has been treated in a number of studies (*2–4, 7, 73*). In our baseline case a maximum hemispherically averaged ozone reduction of ≃ 30 percent is found. This would be substantially smaller if individual warhead yields were all reduced below 1 MT. Considering the relation between solar UV-B radiation increases and ozone decreases (*74*), UV-B doses roughly twice normal are expected in the first year after a baseline exchange (when the dust and soot had dissipated). Large UV-B effects could accompany exchanges involving warheads of greater yield (or large multiburst laydowns).

A variety of toxic gases (pyrotoxins) would be generated in large quantities by nuclear fires, including CO and HCN. According to Crutzen and Birks (*7*), heavy air pollution, including elevated ozone concentrations, could blanket the NH for several months. We are also concerned about dioxins and furans, extremely persistent and toxic compounds which are released during the combustion of widely used synthetic organic chemicals (*75*). Hundreds of tons of dioxins and furans could be generated during a nuclear exchange (*76*). The long-term ecological consequences of such nuclear pyrotoxins seem worthy of further consideration.

Meteorological Perturbations

Horizontal variations in sunlight absorption in the atmosphere, and at the surface, are the fundamental drivers of atmospheric circulation. For many of the cases considered in this study, sizable changes in the driving forces are implied. For example, temperature contrasts greater than 10 K between NH continental areas and adjacent oceans may induce a strong monsoonal circulation, in some ways analogous to the wintertime pattern near the Indian subcontinent. Similarly, the temperature contrast between debris-laden atmospheric regions and adjacent regions not yet filled by smoke and dust will cause new circulation patterns.

Thick clouds of nuclear dust and smoke can thus cause significant climatic perturbations, and related effects, through a variety of mechanisms: reflection of solar radiation to space and absorption of sunlight in the upper atmosphere, leading to overall surface cooling; modification of solar absorption and heating patterns that drive the atmospheric circulation on small scales (*77*) and large scales (*78*); introduction of excess water vapor and cloud condensation nuclei, which affect the formation of clouds and precipitation (*79*); and alteration of the surface albedo by fires and soot (*80*). These effects are closely coupled in determining the overall response of the atmosphere to a nuclear war (*81*). It is not yet possible to forecast in detail the changes in coupled atmospheric circulation and radiation fields, and in weather and microclimates, which would accompany the massive dust and smoke injections treated here. Hence speculation must be limited to the most general considerations.

Water evaporation from the oceans is a continuing source of moisture for the marine boundary layer. A heavy semipermanent fog or haze layer might blanket large bodies of water. The consequences for marine precipitation are not clear, particularly if normal prevailing winds are greatly modified by the perturbed solar driving force. Some continental zones might be subject to continuous snowfall for several months (*10*). Precipitation can lead to soot removal, although this process may not be very efficient for nuclear clouds (*77, 79*). It is likely that, on average, precipitation rates would be generally smaller than in the ambient atmosphere; the major remaining energy source available for storm genesis is the latent heat from ocean evaporation, and the upper atmosphere is warmer than the lower atmosphere which suppresses convection and rainfall.

Despite possible heavy snowfalls, it is unlikely that an ice age would be triggered by a nuclear war. The period of cooling (≲ 1 year) is probably too short to overcome the considerable inertia in the earth's climate system. The oceanic heat reservoir would probably force the climate toward contemporary norms in the years after a war. The CO_2 input from nuclear fires is not significant climatologically (*7*).

Interhemispheric Transport

In earlier studies it was assumed that significant interhemispheric transport of nuclear debris and radioactivity requires a year or more (*2*). This was based on observations of transport under ambient conditions, including dispersion of debris clouds from individual atmospheric nuclear weapons tests. However, with dense clouds of dust and smoke produced by thousands of nearly simultaneous explosions, large dynamical disturbances would be expected in the aftermath of a nuclear war. A rough analogy can be drawn with the evolution of global-scale dust storms on Mars. The lower martian atmosphere is similar in density to the earth's stratosphere, and the period of rotation is almost identical to the earth's (although the solar insolation is only half the terrestrial value). Dust storms that develop in one hemisphere on Mars often rapidly intensify and spread over the entire planet, crossing the equator in a mean time of ≃ 10 days (*15, 82, 83*). The explanation apparently lies in the heating of the dust aloft, which then dominates other heat sources and drives the circulation. Haberle *et al.* (*82*) used a two-dimensional model to simulate the evolution of martian dust storms and found that dust at low latitudes, in the core of the Hadley circulation, is the most important in modifying the winds. In a nuclear exchange, most of the dust and smoke would be injected at middle latitudes. However, Haberle *et al.* (*82*) could not treat planetary-scale waves in their calculations. Perturbations of planetary wave amplitudes may be critical in the transport of nuclear war debris between middle and low latitudes.

Significant atmospheric effects in the SH could be produced (i) through dust and smoke injection resulting from explosions on SH targets, (ii) through transport of NH debris across the meteorological equator by monsoon-like winds (*84*), and (iii) through interhemispheric transport in the upper tropo-

sphere and stratosphere, driven by solar heating of nuclear dust and smoke clouds. Photometric observations of the El Chichón volcanic eruption cloud (origin, 14°N) by the Solar Mesosphere Explorer satellite show that 10 to 20 percent of the stratospheric aerosol had been transported to the SH after ≃ 7 weeks (*85*).

Discussion and Conclusions

The studies outlined here suggest severe long-term climatic effects from a 5000-MT nuclear exchange. Despite uncertainties in the amounts and properties of the dust and smoke produced by nuclear detonations, and the limitations of models available for analysis, the following tentative conclusions may be drawn.

1) Unlike most earlier studies [for instance, (*2*)], we find that a global nuclear war could have a major impact on climate—manifested by significant surface darkening over many weeks, subfreezing land temperatures persisting for up to several months, large perturbations in global circulation patterns, and dramatic changes in local weather and precipitation rates—a harsh "nuclear winter" in any season. Greatly accelerated interhemispheric transport of nuclear debris in the stratosphere might also occur, although modeling studies are needed to quantify this effect. With rapid interhemispheric mixing, the SH could be subjected to large injections of nuclear debris soon after an exchange in the Northern Hemisphere. In the past, SH effects have been assumed to be minor. Although the climate disturbances are expected to last more than a year, it seems unlikely that a major long-term climatic change, such as an ice age, would be triggered.

2) Relatively large climatic effects could result even from relatively small nuclear exchanges (100 to 1000 MT) if urban areas were heavily targeted, because as little as 100 MT is sufficient to devastate and burn several hundred of the world's major urban centers. Such a low threshold yield for massive smoke emissions, although scenario-dependent, implies that even limited nuclear exchanges could trigger severe aftereffects. It is much less likely that a 5000- to 10,000-MT exchange would have only minor effects.

3) The climatic impact of sooty smoke from nuclear fires ignited by airbursts is expected to be more important than that of dust raised by surface bursts (when both effects occur). Smoke absorbs sunlight efficiently, whereas soil dust is generally nonabsorbing. Smoke particles are extremely small (typically < 1 μm in radius), which lengthens their atmospheric residence time. There is also a high probability that nuclear explosions over cities, forests, and grasslands will ignite widespread fires, even in attacks limited to missile silos and other strategic military targets.

4) Smoke from urban fires may be more important than smoke from collateral forest fires for at least two reasons: (i) in a full-scale exchange, cities holding large stores of combustible materials are likely to be attacked directly; and (ii) intense fire storms could pump smoke into the stratosphere, where the residence time is a year or more.

5) Nuclear dust can also contribute to the climatic impact of a nuclear exchange. The dust-climate effect is very sensitive to the conduct of the war; a smaller effect is expected when lower yield weapons are deployed and airbursts dominate surface land bursts. Multiburst phenomena might enhance the climatic effects of nuclear dust, but not enough data are available to assess this issue.

6) Exposure to radioactive fallout may be more intense and widespread than predicted by empirical exposure models, which neglect intermediate fallout extending over many days and weeks, particularly when unprecedented quantities of fission debris are released abruptly into the troposphere by explosions with submegaton yields. Average NH mid-latitude whole-body gamma-ray doses of up to 50 rads are possible in a 5000-MT exchange; larger doses would accrue within the fallout plumes of radioactive debris extending hundreds of kilometers downwind of targets. These estimates neglect a probably significant internal radiation dose due to biologically active radionuclides.

7) Synergisms between long-term nuclear war stresses—such as low light levels, subfreezing temperatures, exposure to intermediate time scale radioactive fallout, heavy pyrogenic air pollution, and UV-B flux enhancements—aggravated by the destruction of medical facilities, food stores, and civil services, could lead to many additional fatalities, and could place severe stresses on the global ecosystem. An assessment of the possible long-term biological consequences of the nuclear war effects quantified in this study is made by Ehrlich *et al.* (*86*).

Our estimates of the physical and chemical impacts of nuclear war are necessarily uncertain because we have used one-dimensional models, because the data base is incomplete, and because the problem is not amenable to experimental investigation. We are also unable to forecast the detailed nature of the changes in atmospheric dynamics and meteorology implied by our nuclear war scenarios, or the effect of such changes on the maintenance or dispersal of the initiating dust and smoke clouds. Nevertheless, the magnitudes of the first-order effects are so large, and the implications so serious, that we hope the scientific issues raised here will be vigorously and critically examined.

References and Notes

1. J. Hampson, *Nature (London)* **250**, 189 (1974).
2. National Academy of Sciences, *Long-Term Worldwide Effects of Multiple Nuclear-Weapon Detonations* (Washington, D.C., 1975).
3. R. C. Whitten, W. J. Borucki, R. P. Turco, *Nature (London)* **257**, 38 (1975).
4. M. C. MacCracken and J. S. Chang, Eds., *Lawrence Livermore Lab. Rep. UCRL-51653* (1975).
5. J. C. Mark, *Annu. Rev. Nucl. Sci.* **26**, 51 (1976).
6. K. N. Lewis, *Sci. Am.* **241**, 35 (July 1979).
7. P. J. Crutzen and J. W. Birks, *Ambio* **11**, 114 (1982).
8. L. W. Alvarez, W. Alvarez, F. Asaro, H. V. Michel, *Science* **208**, 1095 (1980); W. Alvarez, F. Asaro, H. V. Michel, L. W. Alvarez, *ibid.* **216**, 886 (1982); W. Alvarez, L. W. Alvarez, F. Asaro, H. V. Michel, *Geol. Soc. Am. Spec. Pap. 190* (1982), p. 305.
9. R. Ganapathy, *Science* **216**, 885 (1982).
10. O. B. Toon *et al.*, *Geol. Soc. Am. Spec. Pap. 190* (1982), p. 187; J. B. Pollack, O. B. Toon, T. P. Ackerman, C. P. McKay, R. P. Turco, *Science* **219**, 287 (1983).
11. Under the sponsorship of the Defense Nuclear Agency, the National Research Council (NRC) of the National Academy of Sciences has also undertaken a full reassessment of the possible climatic effects of nuclear war. The present analysis was stimulated, in part, by earlier NRC interest in a preliminary estimate of the climatic effects of nuclear dust.
12. Office of Technology Assessment, *The Effects of Nuclear War* (OTA-NS-89, Washington, D.C., 1979).
13. J. E. Coggle and P. J. Lindop, *Ambio* **11**, 106 (1982).
14. S. Bergstrom *et al.*, "Effects of nuclear war on health and health services," *WHO Publ. A36.12* (1983).
15. R. P. Turco, O. B. Toon, T. P. Ackerman, J. B. Pollack, C. Sagan, in preparation.
16. R. P. Turco, P. Hamill, O. B. Toon, R. C. Whitten, C. S. Kiang, *J. Atmos. Sci.* **36**, 699 (1979); *NASA Tech. Pap. 1362* (1979); R. P. Turco, O. B. Toon, P. Hamill, R. C. Whitten, *J. Geophys. Res.* **86**, 1113 (1981); R. P. Turco, O. B. Toon, R. C. Whitten, *Rev. Geophys. Space Phys.* **20**, 233 (1982); R. P. Turco, O. B. Toon, R. C. Whitten, P. Hamill, R. G. Keesee, *J. Geophys. Res.* **88**, 5299 (1983).
17. O. B. Toon, R. P. Turco, P. Hamill, C. S. Kiang, R. C. Whitten, *J. Atmos. Sci.* **36**, 718 (1979); *NASA Tech. Pap. 1363* (1979).
18. O. B. Toon and T. P. Ackerman, *Appl. Opt.* **20**, 3657 (1981); T. P. Ackerman and O. B. Toon, *ibid.*, p. 3661; J. N. Cuzzi, T. P. Ackerman, L. C. Helme, *J. Atmos. Sci.* **39**, 917 (1982).
19. Prediction of circulation anomalies and attendant changes in regional weather patterns requires an appropriately designed three-dimensional general circulation model with at least the following features: horizontal resolution of 10° or better, high vertical resolution through the troposphere and stratosphere, cloud and precipitation parameterizations that allow for excursions well outside present-day experience, ability to transport dust and smoke particles, an interactive radiative transport scheme to calculate dust and smoke effects on light fluxes and heating rates, allowance for changes in particle sizes with time and for wet and dry deposition, and possibly a treatment of the coupling between surface winds and ocean currents and temperatures. Even if such a model were available today, it would not be able to resolve questions of patchiness on horizontal scales of less than several hundred kilometers, of local-

ized perturbations in boundary-layer dynamics, or of mesoscale dispersion and removal of dust and smoke clouds.
20. Advisors, *Ambio* **11**, 94 (1982).
21. R. T. Pretty, Ed., *Jane's Weapon Systems, 1982–1983* (Jane's, London, 1982).
22. *The Military Balance 1982–1983* (International Institute for Strategic Studies, London, 1982).
23. *World Armaments and Disarmament*, Stockholm International Peace Research Institute Yearbook 1982 (Taylor & Francis, London, 1982).
24. R. Forsberg, *Sci. Am.* **247**, 52 (November 1982).
25. The unprecedented difficulties involved in controlling a limited nuclear exchange are discussed by, for example, P. Bracken and M. Shubik [*Technol. Soc.* **4**, 155 (1982)] and by D. Ball [*Adelphi Paper 169* (International Institute for Strategic Studies, London, 1981)].
26. G. Kemp, *Adelphi Paper 106* (International Institute for Strategic Studies, London, 1974).
27. S. Glasstone and P. J. Dolan, Eds., *The Effects of Nuclear Weapons* (Department of Defense, Washington, D.C., 1977).
28. The areas cited are subject to peak overpressures $\geq$ 10 to 20 cal/cm^2.
29. A 1-MT surface explosion ejects $\sim 5 \times 10^6$ tons of debris, forming a large crater (*27*). Typical soils consist of $\simeq$ 5 to 25 percent by weight of grains $\leq$ 1 μm in radius [G. A. D'Almeida and L. Schutz, *J. Climate Appl. Meteorol.* **22**, 233 (1983); G. Rawson, private communication]. However, the extent of disaggregation of the soil into parent grain sizes is probably $\leq$ 10 percent [R. G. Pinnick, G. Fernandez, B. D. Hinds, *Appl. Opt.* **22**, 95 (1983)] and would depend in part on soil moisture and compaction.
30. A 1-MT surface explosion vaporizes $\simeq 2 \times 10^4$ to 4×10^4 tons of soil (*27*), which is ingested by the fireball. Some silicates and other refractory materials later renucleate into fine glassy spheres [M. W. Nathans, R. Thews, I. J. Russell, *Adv. Chem. Ser.* **93**, 360 (1970)].
31. A 1-MT surface explosion raises significant quantities of dust over an area of $\geq$ 100 km^2 by "popcorning," due to thermal radiation, and by saltation, due to pressure winds and turbulence (*27*). Much of the dust is sucked up by the afterwinds behind the rising fireball. Size sorting should favor greatest lifting for the finest particles. The quantity of dust lofted would be sensitive to soil type, moisture, compaction, vegetation cover, and terrain. Probably $> 1 \times 10^5$ tons of dust per megaton can be incorporated into the stabilized clouds in this manner.
32. R. G. Gutmacher, G. H. Higgins, H. A. Tewes, *Lawrence Livermore Lab. Rep. UCRL-14397* (1983); J. Carpenter, private communication.
33. M. W. Nathans, R. Thews, I. J. Russell [in (*30*)]. These data suggest number size distributions that are log-normal at small sizes ($\leq$ 3 μm) and power law ($r^{-\alpha}$) at larger sizes. Considering data from a number of nuclear tests, we adopted an average log-normal mode radius of 0.25 μm, $\sigma = 2.0$, and an exponent, $\alpha = 4$ (*15*). If all particles in the stabilized clouds have radii in the range 0.01 to 1000 μm, the adopted size distribution has $\simeq$ 8 percent of the total mass in particles $\leq$ 1 μm in radius; this fraction of the stabilized cloud mass represents $\leq$ 0.5 percent of the total ejecta and sweep-up mass of a surface explosion and amounts to $\simeq$ 25 tons per kiloton of yield.
34. Atmospheric dust from volcanic explosions differs in several important respects from that produced by nuclear explosions. A volcanic eruption represents a localized dust source, while a nuclear war would involve thousands of widely distributed sources. The dust mass concentration in stabilized nuclear explosion clouds is low ($\leq$ 1 g/m^3), while volcanic eruption columns are so dense they generally collapse under their own weight [G. P. L. Walker, *J. Volcanol. Geotherm. Res.* **11**, 81 (1981)]. In the dense volcanic clouds particle agglomeration, particularly under the influence of electrical charge, can lead to accelerated removal by sedimentation [S. N. Carey and H. Sigurdsson, *J. Geophys. Res.* **87**, 7061 (1982); S. Brazier *et al.*, *Nature (London)* **301** 115 (1983)]. The size distribution of volcanic ash is also fundamentally different from that of nuclear dust [W. I. Rose *et al.*, *Am. J. Sci.* **280**, 671 (1980)], because the origins of the particles are so different. The injection efficiency of nuclear dust into the stratosphere by megaton-yield explosions is close to unity, while the injection efficiency of fine volcanic dust appears to be very low (*15*). For these reasons and others, the observed climatic effects of major historical volcanic eruptions cannot be used, as in (*2*), to calibrate the potential climatic effect of nuclear dust merely by scaling energy or soil volume. However, in cases where the total amount of submicrometer volcanic material that remained in the stratosphere could be determined, climate models have been applied and tested [J. B. Pollack *et al.*, *J. Geophys. Res.* **81**, 1071 (1976)]. We used such a model in this study to predict the effects of specific nuclear dust injections.
35. E. Ishikawa and D. L. Swain, Translators, *Hiroshima and Nagasaki: The Physical, Medical and Social Effects of the Atomic Bombings* (Basic Books, New York, 1981).
36. At Hiroshima, a weapon of roughly 13 KT created a fire over $\simeq$ 13 km^2. At Nagasaki, where irregular terrain inhibited widespread fire ignition, a weapon of roughly 22 KT caused a fire over $\simeq$ 7 km^2. These two cases suggest that low-yield ($\leq$ 1-MT) nuclear explosions can readily ignite fires over an area of $\simeq$ 0.3 to 1.0 km^2/KT—roughly the area contained within the $\simeq$ 10 cal/cm^2 and the $\simeq$ 2 psi overpressure contours (*27*).
37. A. Broido, *Bull. At. Sci.* **16**, 409 (1960).
38. C. F. Miller, "Preliminary evaluation of fire hazards from nuclear detonations," *SRI (Stanford Res. Inst.) Memo. Rep. Project IMU-4021-302* (1962).
39. R. U. Ayers, *Environmental Effects of Nuclear Weapons* (HI-518-RR, Hudson Institute, New York, 1965), vol. 1.
40. S. B. Martin, "The role of fire in nuclear warfare," *United Research Services Rep. URS-764 (DNA 2692F)* (1974).
41. *DCPA Attack Environment Manual* (Department of Defense, Washington, D.C., 1973), chapter 3.
42. *FEMA Attack Environment Manual* (CPG 2-1A3, Federal Emergency Management Agency, Washington, D.C., 1982), chapter 3.
43. H. L. Brode, "Large-scale urban fires," *Pacific Sierra Res. Corp. Note 348* (1980).
44. D. A. Larson and R. D. Small, "Analysis of the large urban fire environment," *Pacific Sierra Res. Corp. Rep. 1210* (1982).
45. Urban and suburban areas of cities with populations exceeding 100,000 (about 2300 worldwide) are surveyed in (*15*). Also discussed are global reserves of flammable substances, which are shown to be roughly consistent with known rates of production and accumulation of combustible materials. P. J. Crutzen and I. E. Galbally (in preparation) reach similar conclusions about global stockpiles of combustibles.
46. Smoke emission data for forest fires are reviewed by D. V. Sandberg, J. M. Pierovich, D. G. Fox, and E. W. Ross ["Effects of fire on air," *U.S. Forest Serv. Tech. Rep. WO-9* (1979)]. Largest emission factors occur in intense large-scale fires where smoldering and flaming exist simultaneously, and the oxygen supply may be limited over part of the burning zone. Smoke emissions from synthetic organic compounds would generally be larger than those from forest fuels [C. P. Bankston, B. T. Zinn, R. F. Browner, E. A. Powell, *Combust. Flame* **41**, 273 (1981)].
47. Sooty smoke is a complex mixture of oils, tars, and graphitic (or elemental) carbon. Measured benzene-soluble mass fractions of wildfire smokes fall in the range $\simeq$ 40 to 75 percent [D. V. Sandberg *et al.* in (*46*)]. Most of the residue is likely to be brown to black (the color of smoke ranges from white, when large amounts of water vapor are present, to yellow or brown, when oils predominate, to gray or black, when elemental carbon is a major component).
48. A. Tewarson, in *Flame Retardant Polymeric Material*, M. Lewin, S. M. Atlas, E. M. Pierce, Eds. (Plenum, New York, 1982), vol. 3, pp. 97–153. In small laboratory burns of a variety of synthetic organic compounds, emissions of "solid" materials (which remained on collection filters after baking at 100°C for 24 hours) ranged from $\simeq$ 1 to 15 percent by weight of the carbon consumed; of low-volatility liquids, $\simeq$ 2 to 35 percent; and of high-volatility liquids, $\simeq$ 1 to 40 percent. Optical extinction of the smoke generated by a large number of samples varied from $\simeq$ 0.1 to 1.5 m^2 per gram of fuel burned.
49. In wildfires, the particle number mode radius is typically about 0.05 μm [D. V. Sandberg *et al.*, in (*46*)]. For burning synthetics the number mode radius can be substantially greater, but a reasonable average value is 0.1 μm [C. P. Bankston *et al.*, in (*46*)]. Often, larger debris particles and firebrands are swept up by powerful fire winds, but they have short atmospheric residence times and are not included in the present estimates (C. K. McMahon and P. W. Ryan, paper presented at the 69th Annual Meeting, Air Pollution Control Association, Portland, Ore., 27 June to 1 July 1976). Nevertheless, because winds exceeding 100 km/hour may be generated in large-scale fires, significant quantities of fine noncombustible surface dust and explosion debris (such as pulverized plaster) might be lifted in addition to the smoke particles.
50. This assumes an average graphitic carbon mass fraction of about 30 to 50 percent, for a pure carbon imaginary refractive index of 0.6 to 1.0 [J. T. Twitty and J. A. Weinman, *J. Appl. Meteorol.* **10**, 725 (1971); S. Chippett and W. A. Gray, *Combust. Flame* **31**, 149 (1978)]. The real part of the refractive index of pure carbon is 1.75, and for many oils is 1.5 to 1.6. Smoke particles were assigned an average density of 1 g/cm^3 (C. K. McMahon, paper presented at the 76th Annual Meeting, Air Pollution Control Association, Atlanta, Ga., 19 to 24 June 1983). Solid graphite has a density $\simeq$ 2.5 g/cm^3, and most oils, $\lesssim$ 1 g/cm^3.
51. A number of targets with military, economic, or political significance can also be identified in tropical northern latitudes and in the SH (*20*).
52. Attenuation of direct sunlight by dust and smoke particles obeys the law $I/I_0 = \exp(-\tau/\mu_0)$, where τ is the total extinction optical depth due to photon scattering and absorption by the particles and μ_0 is the cosine of the solar zenith angle. The optical depth depends on the wavelength of the light and the size distribution and composition of the particles, and is generally calculated from Mie theory (assuming equivalent spherical particles). The total light intensity at the ground consists of a direct component and a diffuse, or scattered, component, the latter usually calculated with a radiative transfer model. The extinction optical depth can be written as $\tau = XML$, where X is the specific cross section (m^2/g particulate), M the suspended particle mass concentration (g/m^3), and L the path length (m). It is the sum of a scattering and an absorption optical depth ($\tau = \tau_s + \tau_a$). Fine dust and smoke particles have scattering coefficients $X_s \cong 3$ to 5 m^2/g at visible wavelengths. However, the absorption coefficients X_a are very sensitive to the imaginary part of the index of refraction. For typical soil particles, $X_a \lesssim 0.1$ m^2/g. For smokes, X_a can vary from $\sim$ 0.1 to 10 m^2/g, roughly in proportion to the volume fraction of graphite in the particles. Occasionally, specific extinction coefficients for smoke are given relative to the mass of fuel burned; then X implicitly includes a multiplicative emission factor (grams of smoke generated per gram of fuel burned).
53. R. P. Turco, O. B. Toon, R. C. Whitten, P. Hamill, *Eos* **63**, 901 (1982).
54. J. A. Ogren, in *Particulate Carbon: Atmospheric Life Cycle*, G. T. Wolff and R. L. Klimisch, Eds. (Plenum, New York; 1982), pp. 379–391.
55. To estimate the wildfire area, we assume that 25 percent of the total nonurban yield, or 1000 MT, ignites fires over an area of 500 km^2/MT—approximately the zone irradiated by 10 cal/cm^2—and that the fires do not spread outside this zone (*39*). R. E. Huschke [*Rand Corp. Rep. RM-5073-TAB* (1966)] analyzed the simultaneous flammability of wildland fuels in the United States, and determined that about 50 percent of all fuels are at least moderately flammable throughout the summer months. Because $\simeq$ 50 percent of the land areas of the countries likely to be involved in a nuclear exchange are covered by forest and brush, which are flammable about 50 percent of the time, the 1000-MT ignition yield follows statistically.
56. Most of the background smoke is injected into the lowest 1 to 2 km of the atmosphere, where it has a short lifetime, and consists on the average of $\leq$ 10 percent graphitic carbon [R. P. Turco, O. B. Toon, R. C. Whitten, J. B. Pollack, P. Hamill, in *Precipitation Scavenging, Dry Deposition and Resuspension*, H. R. Pruppacher, R. G. Semonin, W. G. N. Slinn, Eds. (Elsevier, New York, 1983), p. 1337]. Thus, the average optical depth of ambient atmospheric soot is only $\leq$ 1 percent of the initial optical depth of the baseline nuclear war smoke pall.
57. H. E. Landsberg and J. M. Albert, *Weatherwise* **27**, 63 (1974).
58. H. Stommel and E. Stommel, *Sci. Am.* **240**, 176 (June 1979).
59. O. B. Toon and J. B. Pollack, *Nat. Hist.* **86**, 8 (January 1977).
60. H. H. Lamb, *Climate Present, Past and Future* (Methuen, London, 1977), vols. 1 and 2.
61. Notwithstanding possible alterations in the surface albedo due to the fires and deposition of soot (*15, 80*).
62. S. G. H. Philander, *Nature (London)* **302**, 295 (1983); B. C. Weare, *Science* **221**, 947 (1983).
63. D. H. Milne and C. P. McKay, *Geol. Soc. Am. Spec. Pap. 190* (1982), p. 297.
64. O. B. Toon, *Eos* **63**, 901 (1982).
65. The stratosphere is normally defined as the region of constant or increasing temperature with increasing height lying just above the tropo-

sphere. The residence time of fine particles in the stratosphere is considerably longer than in the upper troposphere because of the greater stability of the stratospheric air layers and the absence of precipitation in the stratosphere. With large smoke injections, however, the ambient temperature profile would be substantially distorted (for instance, see Fig. 3) and a "stratosphere" might form in the vicinity of the smoke cloud, increasing its residence time at all altitudes (*15*). Thus the duration of sunlight attenuation and temperature perturbations in Figs. 1 to 6 may be considerably underestimated.

66. Transport of soot from the boundary layer into the overlying free troposphere can occur by diurnal expansion and contraction of the boundary layer, by large-scale advection, and by strong localized convection.
67. F. Barnaby and J. Rotblat, *Ambio* **11**, 84 (1982).
68. The term "intermediate" fallout distinguishes the radioactivity deposited between several days and ~ 1 month after an exchange from "prompt" fallout ($\lesssim$ 1 day) and "late" fallout (months to years). Intermediate fallout is expected to be at least hemispheric in scale and can still deliver a significant chronic whole-body gamma-ray dose. It may also contribute a substantial internal dose, for example, from ^{131}I. The intermediate time scale gamma-ray dose represents, in one sense, the minimum average exposure far from targets and plumes of prompt fallout. However, the geographic distribution of intermediate fallout would still be highly variable, and estimates of the average dose made with a one-dimensional model are greatly idealized. The present calculations were calibrated against the observed prompt fallout of nuclear test explosions (*15*).
69. There is also reason to believe that the fission yield fraction of nuclear devices may be increasing as warhead yields decrease and uranium processing technology improves. If the fission fraction were unity, our dose estimates would have to be doubled. We also neglect additional potential sources of radioactive fallout from salted "dirty" weapons and explosions over nuclear reactors and fuel reprocessing plants.
70. J. Knox (*Lawrence Livermore Lab. Rep. UCRL-89907*, in press) reports fallout calculations which explicitly account for horizontal spreading and transport of nuclear debris clouds. For a 5300-MT strategic exchange, Knox computes average whole-body gamma-ray doses of 20 rads from 40° to 60°N, with smaller average doses elsewhere. Hot spots of up to 200 rads over areas of ~ 10^6 km^2 are also predicted for intermediate time scale fallout. These calculations are consistent with our estimates.
71. H. Lee and W. E. Strope [*Stanford Res. Inst. Rep. EGU 2981* (1974)] studied U.S. exposure to transoceanic fallout generated by several assumed Sino-Soviet nuclear exchanges. Taking into account weathering of fallout debris, protection by shelters, and a 5-day delay before initial exposure, potential whole-body gamma-ray doses $\lesssim$ 10 rads and internal doses $\gtrsim$ 10 to 100 rads, mainly to the thyroid and intestines, were estimated.
72. These estimates assume normal rates and patterns of precipitation, which control the intermediate time scale radioactive fallout. In severely perturbed cases, however, it may happen that the initial dispersal of the airborne radioactivity is accelerated by heating, but that intermediate time scale deposition is suppressed by lack of precipitation over land.
73. H. Johnston, G. Whitten, J. Birks, *J. Geophys. Res.* **78**, 6107 (1973); H. S. Johnston, *ibid.* **82**, 3119 (1977).
74. S. A. W. Gerstl, A. Zardecki, H. L. Wiser, *Nature (London)* **294**, 352 (1981).
75. M. P. Esposito, T. O. Tiernan, F. E. Dryden, *U.S. EPA Rep. EPA-600/280-197* (1980).
76. J. Josephson, *Environ. Sci. Technol.* **17**, 124A (1983). In burning of PCB's, for example, release of toxic polycyclic chlorinated organic compounds can amount to 0.1 percent by weight. In the United States more than 300,000 tons of PCB's are currently in use in electrical systems [S. Miller, *Environ. Sci. Technol.* **17**, 11A (1983)].
77. C.-S. Chen and H. D. Orville [*J. Appl. Meteorol.* **16**, 401 (1977)] model the effects of fine graphitic dust on cumulus-scale convection. They show that strong convective motions can be established in still air within 10 minutes after the injection of a kilometer-sized cloud of submicrometer particles of carbon black, at mixing ratios $\lesssim$ 50 ppb by mass. Addition of excess humidity in their model to induce rainfall results in still stronger convection; the carbon dust is raised higher and spread farther horizontally, while $\lesssim$ 20 percent is scavenged by the precipitation. W. M. Gray, W. M. Frank, M. L. Corrin, and C. A. Stokes [*J. Appl. Meteorol.* **15**, 355 (1976)] discuss possible mesoscale ($\gtrsim$ 100 km) weather modifications due to large carbon dust injections.
78. C. Covey, S. Schneider, and S. Thompson (in preparation) report GCM simulations which include soot burdens similar to those in our baseline case. They find major perturbations in the global circulation within a week of injection, with strong indications that some of the nuclear debris at northern mid-latitudes would be transported upward and toward the equator.
79. R. C. Eagan, P. V. Hobbs, L. F. Radke, *J. Appl. Meteorol.* **13**, 553 (1974).
80. C. Sagan, O. B. Toon, and J. B. Pollack [*Science* **206**, 1363 (1979)] discuss the impact of anthropogenic albedo changes on global climate. Nuclear war may cause albedo changes by burning large areas of forest and grassland; by generating massive quantities of soot which can settle out on plants, snowfields, and ocean surface waters; and by altering the pattern and extent of ambient water clouds. The nuclear fires in the baseline case consume an area $\approx 7.5 \times 10^5$ km^2, or only $\approx$ 0.5 percent of the global landmass; it is doubtful that an albedo variation over such a limited area is significant. All the soot in the baseline nuclear war case, if spread uniformly over the earth, would amount to a layer ~0.5 μm thick. Even if the soot settled out uniformly on all surfaces, the first rainfall would wash it into soils and watersheds. The question of the effect of soot on snow and ice fields is under debate (J. Birks, private communication). In general, soot or sand accelerates the melting of snow and ice. Soot that settles in the oceans would be rapidly removed by nonselective filter-feeding plankton, if these survived the initial darkness and ionizing radiation.
81. In the present calculations, chemical changes in stratospheric O_3 and NO_2 concentrations cause a small average temperature perturbation compared to that caused by nuclear dust and smoke; it seems unlikely that chemically induced climatic disturbances would be a major factor in a nuclear war. Tropospheric ozone concentrations, if tripled (*7*), would lead to a small greenhouse warming of the surface [W. C. Wang, Y. L. Yung, A. A. Lacis, T. Mo, J. E. Hansen, *Science* **194**, 685 (1976)]. This might result in more rapid surface temperature recovery. However, the tropospheric O_3 increase is transient (~ 3 months in duration) and probably secondary in importance to the contemporaneous smoke and dust perturbations.
82. R. M. Haberle, C. B. Leovy, J. B. Pollack, *Icarus* **50**, 322 (1983).
83. During the martian dust storm of 1971–1972, the IRIS experiment on Mariner 9 observed that suspended particles heated the atmosphere and produced a vertical temperature gradient that was substantially subadiabatic [R. B. Hanel *et al.*, *Icarus* **17**, 423 (1972); J. B. Pollack *et al.*, *J. Geophys. Res.* **84**, 2929 (1979)].
84. V. V. Alexandrov, private communication; S. H. Schneider, private communication.
85. G. E. Thomas, B. M. Jakosky, R. A. West, R. W. Sanders, *Geophys. Res. Lett.* **10**, 997 (1983); J. B. Pollack *et al.*, *ibid.*, p. 989; B. M. Jakosky, private communication.
86. P. Ehrlich *et al.*, *Science* **222**, 1293 (1983).
87. H. M. Foley and M. A. Ruderman, *J. Geophys. Res.* **78**, 4441 (1973).
88. We gratefully acknowledge helpful discussions with J. Berry, H. A. Bethe, C. Billings, J. Birks, H. Brode, R. Cicerone, L. Colin, P. Crutzen, R. Decker, P. J. Dolan, P. Dyal, F. J. Dyson, P. Ehrlich, B. T. Feld, R. L. Garwin, F. Gilmore, L. Grinspoon, M. Grover, J. Knox, A. Kuhl, C. Leovy, M. MacCracken, J. Mahlman, J. Marcum, P. Morrison, E. Patterson, R. Perret, G. Rawson, J. Rotblat, E. E. Salpeter, S. Soter, R. Speed, E. Teller, and R. Whitten on a variety of subjects related to this work. S. H. Schneider, C. Covey, and S. Thompson of the National Center for Atmospheric Research generously shared with us preliminary GCM calculations of the global weather effects implied by our smoke emissions. We also thank the almost 100 participants of a 5-day symposium held in Cambridge, Mass., 22 to 26 April, for reviewing our results; that symposium was organized by the Conference on the Longterm Worldwide Biological Consequences of Nuclear War under a grant from the W. Alton Jones Foundation. Special thanks go to Janet M. Tollas for compiling information on world urbanization, to May Liu for assistance with computer programming, and to Mary Maki for diligence in preparing the manuscript.